

# Large-Scale Noise Characterization of Narrowband Power Line Communications

## Measurements, Analysis and Modeling

Simone Raponi<sup>†</sup>, Javier Hernandez<sup>\*†</sup>, Aymen Omri<sup>\*</sup>, and Gabriele Oligeri<sup>†</sup>

<sup>\*</sup>Iberdrola Innovation Middle East, Doha, Qatar.

<sup>†</sup>Division of Information and Computing Technology (ICT),  
College of Science and Engineering (CSE),  
Hamad Bin Khalifa University (HBKU)

**Abstract**—Noise modeling in power line communications has recently drawn the attention of researchers. However, when characterizing the noise process in narrowband communications, previous works have only focused on small-scale phenomena involving fine-grained details. Nevertheless, the reliability of the communication link is also affected by long-term noise phenomena, that in turn, can be leveraged to maximize transfer rates in higher layers.

This paper introduces the concept of large-scale noise characterization for narrowband power line communications and provides a statistical analysis of the long-term trends of power noise. We introduce a statistical description of the noise process in the large-scale time domain based on real field measurements in the FCC band (10 KHz - 490 KHz). The collected data included more than 1.8 billion samples taken from three different locations over a time period of approximately 10 days. The noise samples were statistically analyzed by considering stationarity, autocorrelation, and independence. Finally, we highlight the presence of time series correlations (up to 30 s) and we prove that the noise level variation can be modeled according to a  $t$ -location scale distribution, that is characterized by fluctuations bounded to  $3dB\mu V$ .

**Index Terms**—NB-PLC, Noise Modeling, Field Measurements, Statistical Analysis.

### I. INTRODUCTION

Power line communication (PLC) is a technology that exploits the already existing power distribution infrastructure to enable communication among devices. Indeed, PLC represents one of the enabling technologies that will pave the way to the migration from old power grids (mainly electromechanical infrastructures devoted to the delivery of power from the producer to the consumers) to the modern smart grid paradigm, which involves several new functionalities and services such as smart metering, electricity trading, and transactive energy.

PLC features significant advantages with respect to standard communication infrastructures (such as wireless radio, fiber optics, or Ethernet) since it exploits an already existing infrastructure—the one adopted for power delivery—and requires minimal maintenance for communication.

PLC is divided into three different categories: Ultra narrowband power line communication (UNB-PLC), Narrowband power line communication (NB-PLC), and Broadband power line communication (BB-PLC) [1], [2]. Smart grid, and in particular smart metering, has found in NB-PLC a natural

partner [3]–[6]. NB-PLC comprises all the communications that take place in the spectrum between 9 and 500 KHz, with small bandwidth requirements due to the higher noise levels that affect such low frequencies. The noise characterization of PLC channels has attracted the attention of many researchers quite recently, and the vast majority of related studies have focused on *small-scale* modeling that involves the analysis of fine-grained phenomena, such as the noise generated by switching home appliances on and off.

In general, small-scale modeling can be categorized into the following families: (i) colored background noise, (ii) narrow-band noise, (iii) periodic impulsive noise (which can be either synchronous or asynchronous with respect to the main frequency), and finally, (iv) asynchronous impulsive noise [7]. In general, colored noise and narrow-band noise are considered to be background noise, while the rest are considered to be impulsive noise. Impulsive noise is the most important source of error affecting communication links. However, impulsive noise is difficult to predict and it may even be as high as 40 dB above the background noise level [8]. Compared with asynchronous impulsive noise that is dominant in broadband PLC, this type of noise contains longer noise bursts that occur periodically with half the AC cycle [9].

We stress that the term “small-scale” refers to the time duration of the phenomena and not to its spectral amplitude. We justify the adoption of this term by recalling the wireless communications domain, where small-scale refers to the rapid changes in the amplitude and phase of a radio signal, while large-scale refers to the average signal power attenuation over large distances [10]. In this paper, we refer to *large-scale* noise characterization as the modeling of the average noise power over long periods, such hours or days. To the best of our knowledge, this paper represents the very first contribution in the area, thus paving the way for further investigation.

While small-scale modeling turns out to be extremely important to guarantee the reliability of communications over NB-PLC channels, in this study we shed light on a completely different aspect, by highlighting the existence of long-term phenomena that can be exploited by higher communication layers to significantly increase the quality of communication. Indeed, driven by the intuition that people daily activities are characterized by long-term periodic cycles (on the order of

hours), we focus our analysis on a larger scale, by considering only the long-term trends of the noise power from three different locations.

**Contribution.** This paper introduces the concept of *large-scale* noise modeling involving the analysis, characterization, and modeling of the noise process in the NB-PLC band over long periods. We collected approximately 10 days of noise power measurements from three different locations in Doha, Qatar, for a total of  $> 1.8$  billion samples (publicly available at the following link [11] when the paper will be accepted for publication). We provided a statistical description of different aspects of noise power involving correlation, independence, and stationarity. Finally, by exploiting the previous statistical results, we provide some insight into modeling and forecasting noise power over long term periods.

**Paper Organization.** The rest of this paper is organized as follows. Section II resumes important related contributions in the literature. Section III presents the measurement setup. The different aspects of noise in the frequency domain are detailed in Section IV. Section V investigates the correlation and the independence of the noise samples. The modeling and forecasting part is presented and detailed in Section VI. Then, a discussion of the results is presented in Section VII. Finally, conclusions are drawn in Section VIII.

## II. RELATED WORK

As mentioned in the introduction, to propose more effective and efficient communication schemes in NB-PLC systems there is a need to study the power lines environment, together with the properties and the characteristics of the communication channels. This would allow better exploiting the communication channel thus increasing the performance of NB-PLC systems. Among the distinctive features of power lines, one that is worth mentioning is time-varying non-white noise, which is defined as the sum of noise waveforms produced by appliances that are connected to the power line network [12]. Refer to [13] for a brief survey of existing noise models for the in-home PLC scenario and to [14] for a brief survey of impulse noise.

One of the first mathematical model of noise in NB-PLC was introduced in [12]. The authors represented noise as a colored cyclostationary Gaussian process whose variance is a periodic time function and whose Power spectral density (PSD) is fitted to the measured noise. The proposed model provides an effective benchmark for designing and evaluating communication systems under a power line noise environment and is considerably different from conventional noise models. However, the proposed model suffers from several limitations because it ignores the time-varying spectral behavior of the noise, it is inappropriate for Orthogonal frequency-division multiplexing (OFDM) systems and only applies to Narrowband (NB) single-carrier systems.

To overcome this limitation, the authors in [15] proposed a cyclostationary noise model for NB-PLC that accounts for both the time and the frequency properties of the measured noise. Specifically, the cyclostationarity period of the NB-PLC noise is partitioned into several temporal regions, each of them

containing the generated noise as a stationary colored Gaussian process. In this way, every region is characterized by a particular PSD, that is fitted to the actual noise measurements. Although the proposed model provides a good fitting for the measured NB-PLC noise, the authors in [16] highlighted two severe drawbacks: (i) instead of relying on a mathematical model, the number of stationary temporal regions (together with the regional boundaries) are inferred by visually inspecting the measured noise spectrogram; and (ii) the noise process within each region is carried out independently of the other regions, thus ignoring any possible cross-correlation between the different noise processes across the regions. To address these drawbacks, in the same study, the authors synthesized the NB-PLC noise samples by relying on a frequency-shift filter, which was designed to shape an input white noise spectrum extracted from the experimental noise measurements. Even by keeping the same computational complexity of [15], the model proposed in [16] exhibited a performance gain in terms of the Normalized mean squared error (NMSE) in the cyclic autocorrelation.

In [8], the authors proposed a simulated noise model that describes the noise affecting a communication system using the OFDM modulation of a power line channel. The proposed model, which is easily implementable in computer simulations, takes account of the statistical properties of the component parameters and depicts the features of both the background and the impulsive noise.

A statistical model for the asynchronous impulsive noise in PLC networks was put forward in [17]. The authors first exploited the physical properties of the PLC network to derive a statistical-physical model of the instantaneous statistics of asynchronous noise, and then validated the distribution by relying on both simulated and measured PLC noise data. Impulsive noise in (indoor) NB-PLC was also studied in [18], in which the authors proposed a stochastic model to provide an accurate characterization. The first phase consisted of extracting both the pulses and their characteristic parameters, which eventually compose four empirical classes. The majority of the pulses were grouped in the first class, which contained single pulses in the form of damped sinusoids with pseudo-frequencies below 500 KHz. Then, the authors determined which distributions most effectively fit the data. According to the study: the pulses pseudo-frequency deduced from the measurements followed a log-normal distributions at three different intervals; the peak amplitude was well fitted by Beta distributions, the duration by Weibull distributions, while the interarrival time was lognormally distributed. Furthermore, the normalized damping factor of the sinusoids follows Gamma distribution, and the phase of the pulses appeared to be normally distributed by absolute value.

The use of the  $\alpha$ -model as an alternative to the Gaussian model to capture PLC background noise was proposed by [9]. The authors provided evidence that the marginal distribution of the noise found in PLC systems exhibits particular statistical properties that can be well modeled by relying on an  $\alpha$ -stable distribution. After presenting a practical application of the model to synthesize noise in the power line, the authors evaluated the performance of an OFDM communication system

TABLE I: Description of the Locations involved in our measurement campaign

	Type	Area ( $m^2$ )	N. of people
Location 1	Apartment	100	4
Location 2	Apartment	260	3
Location 3	Villa	250	1

under both Gaussian and  $\alpha$ -stable background noise. Among their conclusions they pointed out that, when highly impulsive background traffic is (mistakenly) assumed as Gaussian in evaluation models, there is a risk of largely overestimating the performance of the system. It is worth mentioning that the  $\alpha$ -model had already been used by the same authors to describe both the impulsive and the background noise for PLC systems in industrial environments [19].

In addition to the Gaussian model and the  $\alpha$ -model, many other distributions have been introduced to fit the noise data in PLC. Among them, Middleton’s class A distribution [20], the Nagakami-m distribution [21], and the Rayleigh distribution [22] are worth mentioning.

In [23], the authors focused on Middleton’s class A distribution and analyzed its suitability to model noise amplitude in NB-PLC. The analysis was carried out by relying on 311 noise registers measured in the CENELEC-A band. According to the study, the Middleton’s class A distribution exhibits a quite limited capability to represent the measured noise, since only a small percentage of the registers (i.e., 14.47%) presents amplitudes drawn from the distribution.

### III. MEASUREMENT SETUP

Our noise field measurements were performed in the NB-PLC Federal Communications Commission (FCC) band (10 KHz - 490 KHz) and were segmented into eight sub-bands, following the PowerLine Intelligent Metering Evolution (PRIME) standard version 1.4 [24]. The eight channels were within the frequency band from 42 KHz to 471 KHz, where the bandwidth of each channel and the sub-carrier mapping were presented according to PRIME protocol [24].

An evaluation kit for the PL360 modem from Microchip [25], [26] was used to perform the long term NB-PLC noise field measurements. The PL360 is a multi-protocol PLC modem designed with a flexible architecture that allows the implementation of standard and customized PLC solutions [25].

**Locations.** The measuring devices were directly connected to the Low Voltage (LV) lines as close as possible to the electrical meter. Figure 1 shows a PLC modem coupled to a LV three phase power meter for gathering data. A laptop, connected via USB to the measuring device, was used to store the data. The measurements were acquired from three customers’ premises, i.e., Locations 1, 2, and 3 as per Table I.

**Sampling period.** Our measurement campaign lasted for approximately 10 days. The measurements were recorded in  $dB\mu V$  units, with a sampling period of 1 s. We stress that our analysis aimed at highlighting the long-term phenomena of the noise process, i.e., involving hours or days, as presented in Figure 2. Contrary to other contributions, we did not want



Fig. 1: PLC modem coupled to a LV line at the customers meter distribution box.

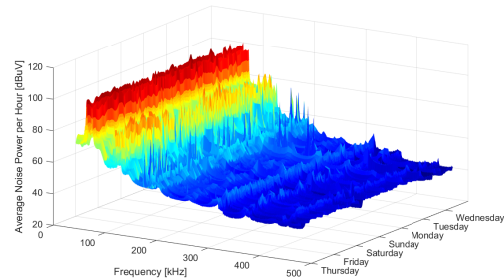


Fig. 2: PLC noise power variation during one week.

to model small scale effects lasting for  $\mu s$ , such as impulsive noise, but we were interested in investigating how the day-to-day human behavior and household appliances affect the noise process on a large-scale time frame.

We performed a preliminary analysis of the collected noise values that highlighted the quality of the sampling process. Figure 3 shows the probability distribution function associated with the time-gap between two consecutive samples. The analysis was performed considering all the noise values from all three locations for a total of 1,826,665,198 samples. We observed that a sampling period of 1s recorded for 1.0655, which introduced an error (delay) of approximately 65ms. We observed other spurious sampling periods that were statistically insignificant as proved by the cumulative distribution function in the inset figure of Fig. 3, i.e., 95% of the sampling periods had an absolute error of less than 0.08 s.

### IV. FREQUENCY DOMAIN

In this section, we consider different aspects of the noise in the frequency domain.

**Spectrum-wise analysis.** Our preliminary analysis consisted of estimating the noise levels ( $dB\mu V$ ) as a function of the frequency spanning between 41,992 and 47,168 Hz. For each frequency, we considered a time series of 639K measurements of the noise (more than one week), and we computed the

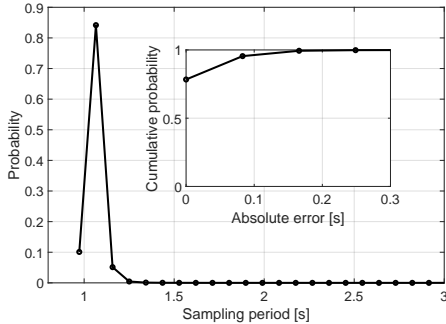


Fig. 3: Probability distribution function associated with the actual sampling period and cumulative probability associated with the absolute error. The sampling procedure is affected by only minor delays, i.e., less than 65ms respect to the requested sampling of 1 sample per second.

minimum, quantiles 10 (q10), 50 (q50), 90 (q90), and finally, the maximum. Figure 4 shows the aforementioned statistics as a function of the considered frequencies. First, we observe that higher frequencies are characterized by lower levels of noise, i.e., there is a clear trend—involving all the statistics—according to which, the level of noise decreases when the frequency increases. We identify the following regions:

- **Region 1 (R1)** [41.9KHz - 95KHz]. In this region, the noise is almost independent of the frequency and characterized by a median value equal to  $68 \text{ dB}\mu\text{V}$ . The difference between quantile 90 and quantile 10 ( $q90 - q10$ ) is approximately  $20 \text{ dB}\mu\text{V}$  across the region, while the overall variance (max-min) sums to  $90 \text{ dB}\mu\text{V}$ . This means that the 80% of the samples are in the tight range of  $\approx 20 \text{ dB}\mu\text{V}$ , while there are a few (less than 20%) samples characterized by high variance, i.e.,  $\approx \pm 30 \text{ dB}\mu\text{V}$ .
- **Region 2 (R2)** [95KHz - 200KHz]. As in the previous case, the noise is (almost) independent of the frequency and is characterized by a median value of approximately  $40 \text{ dB}\mu\text{V}$ , while the  $q90 - q10$  variance is smaller than  $20 \text{ dB}\mu\text{V}$ .
- **Region 3 (R3)** [200KHz - 300KHz]. This region is characterized by a lower level of noise with respect to R1 and R2, i.e., approximately  $30 \text{ dB}\mu\text{V}$  considering the median value (solid green line), although we observe that Location 3 is affected by higher values of noise, i.e., approximately  $39 \text{ dB}\mu\text{V}$  (median value). The overall noise variance ( $q90 - q10$ ) is quite small, i.e.,  $15 \text{ dB}\mu\text{V}$ , while the min-max variance is significantly smaller than in previous cases, being at approximately  $60 \text{ dB}\mu\text{V}$ , which is mainly due to an increased minimum level of noise.
- **Region 4 (R4)** [300KHz - 471.68KHz]. This region is characterized by flat noise with a median value of approximately  $23 \text{ dB}\mu\text{V}$ . The noise variance is about  $10 \text{ dB}\mu\text{V}$ , while the min-max distance is the same as the

one in Region 2 ( $\approx 65 \text{ dB}\mu\text{V}$ ). Finally, we observe a few anomalies in the maximum levels of noise with a period of 55KHz, with spikes of  $22 \text{ dB}\mu\text{V}$  of amplitude.

Figure 5 shows the probability distribution function associated with all the noise values, i.e., considering all samples for all frequencies. The three peaks at 25, 40, and  $65 \text{ dB}\mu\text{V}$  match the average values of the previously introduced regions. Finally, we observe that 80% of the noise values ( $q90 - q10$ ) are in the range between 20 and  $64 \text{ dB}\mu\text{V}$  (inset figure of Fig. 5).

## V. CORRELATION AND INDEPENDENCE OF THE NOISE SAMPLES

In this section, we provide an in-depth analysis about the stationarity and independence of the collected noise samples by taking different tests and statistics into account.

**Stationarity.** We start our analysis by considering first-order statistics. Figure 6 shows a typical sequence (Frequency 1) of noise values (black dots) of approximately 10 days. We considered the mean (red dots), the standard deviation (blue dots), and the variance (magenta dots) over a sliding window of 3600 samples (1 h).

The objective of our analysis was to evaluate the stationarity of the random process associated with the noise. We started our analysis by considering first and second order statistics, i.e., the mean and variance from Fig. 6, which were characterized by minute fluctuations. Conversely, the raw values of the noise were affected by large fluctuations between 13 and  $70 \text{ dB}\mu\text{V}$ , as depicted by the moving variance in Fig. 6. Given the aforementioned considerations, our intuition was that the noise values represented a stationary sequence. We used the Kwiatkowski, Phillips, Schmidt, and Shin (KPSS) test for a unit root in the time series [27]. In our analysis, we consider one subcarrier from each channel and adjacent chunks of different sizes ranging between 30 and 600 samples (0.5 min and 10 min, respectively). For each chunk, we ran the KPSS test, which gave 0 to indicate we should reject the stationary in favor of the unit root alternative, and 1 when the test failed to reject the stationarity. For each chunk size, we evaluated the fraction of stationary chunks by summing the chunks with a test output of 1 with respect to the total number of chunks.

Figure 7 shows the results of our stationarity analysis considering the three locations. The fraction of chunks that are positive for the stationarity test decreases when the length of the chunk becomes larger, i.e., larger chunks are more likely to contain non-stationary sub-sequences. The two chunk extremes, i.e., 0.5 and 10 min, have similar values at location 2 and 3, while locations 1 is characterized by higher levels of stationarity for larger chunks. It is worth noting that the noise process presents a high level of stationarity for large period of time: chunks shorter than 2 min (120 samples) in Location 1 are stationary in the 90% of the cases while, to have similar values in Location 2 and 3, chunks length should be reduced to approximately 30 seconds (30 samples). This result is quite significant because it implies that the noise process is stationary for large amount of time, i.e., between 30 s and 2 min depending on the considered location.

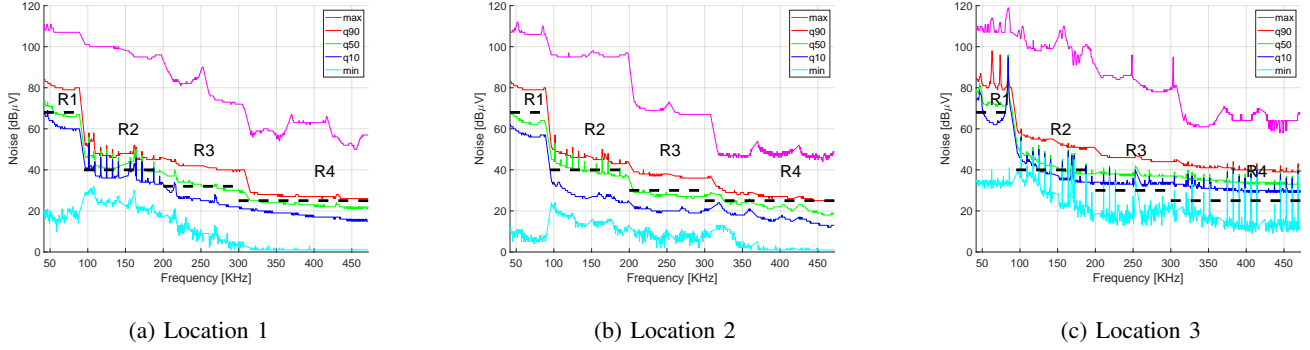


Fig. 4: Noise levels ( $dB\mu V$ ) as a function of the frequency (KHz). We considered three different locations (1, 2, and 3) and more than one week of noise samples taken at 1 sample per second (1Hz). We computed minimum (cyan), maximum (magenta) and quantile 10 (blue), 50 (green), and 90 (red). The dashed black line highlights the four regions (R1, R2, R3, and R4) with similar noise characteristics.

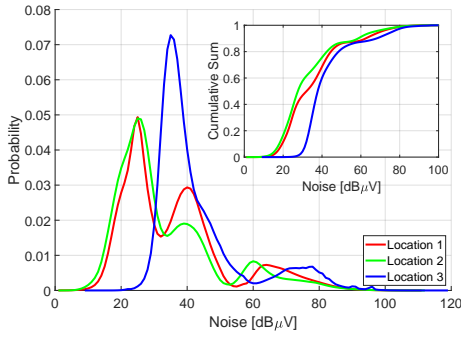


Fig. 5: Probability distribution function associated with all the noise sample values. The inset figure refers to the cumulative distribution function associated with the noise values.

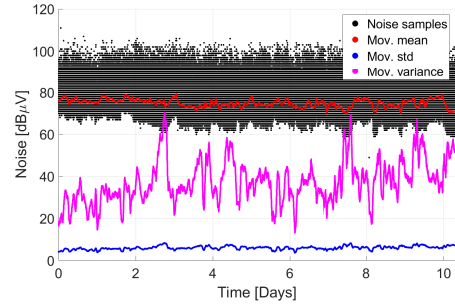


Fig. 6: First/Second-order statistics (moving mean and standard deviation with window size of 1 hour) computed over the noise values of frequency 1.

Finally, we performed a similar analysis with the augmented Dickey-Fuller test and the Phillips-Perron test for one unit root, and we obtained similar results.

**Independence test.** We began our analysis of the independence of the noise samples with the autocorrelation. We computed the AutoCorrelation Function (ACF) up to lag 10 for all the frequencies and considered locations. ACF is the correlation of a signal with a delayed copy of itself as a function of the delay (i.e., lag). ACF is a very important tool because it allows to estimate whether the noise sample at time  $k$  can be expressed (forecast) as a function of the values at previous lags. For each location, we computed the ACF at lags 1, 2, 5, and 10, and we reported them as a function of the frequency in Fig. 8.

Figure 8 shows the autocorrelation function computed over a time span of 3600 lags (1 h).

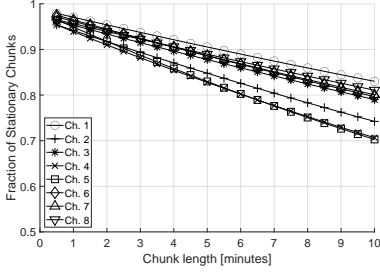
Firstly, we considered the significance bounds, computed from Bartlett's approximation, which yielded:

$$b = \pm \frac{z_{(1-\alpha)/2}}{\sqrt{N}}$$

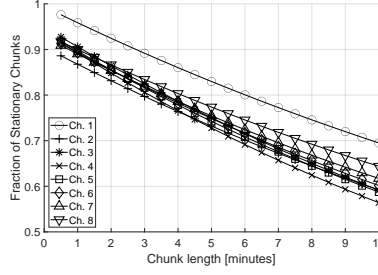
where  $z$  is the quantile of a normal distribution, and  $\alpha = 0.95$  and  $N$  is the length of the trace, yielding  $b = \pm 0.0022$ . If the autocorrelation value is between the lower and the upper bounds, we can infer that there is no correlation at the considered lag and the null hypothesis of independence cannot be rejected at a significance level of  $\alpha$ .

In order to better highlight the behavior of adjacent frequencies, we interpolated the ACF values at lags 1, 2, 5, and 10 with a polynomial fitting curve of high order (20), and we depicted the result of the interpolation using the solid red, green, blue, and cyan colors for lags 1, 2, 5 and 10, respectively.

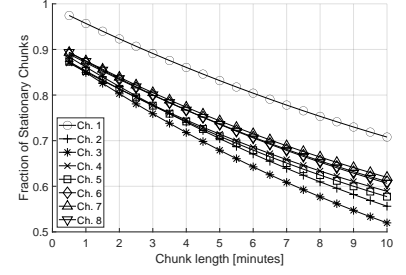
All the locations exhibited different levels of positive correlation for all the considered lags. Firstly, we observed that for all locations, the frequencies belonging to channel 1 showed the smallest correlation values, i.e., 0.1, 0.2, and 0.1 for Locations 1, 2, and 3, respectively. Moreover, the correlation was higher at lag 1, while it became smaller when the lags increased to a value 10. Finally, we observed that frequencies belonging to channels 2, 3, 4, and 5 were characterized by higher correlation values, i.e., approximately 0.5, 0.7 and 0.5, for location 1, 2 and 3, respectively.



(a) Location 1

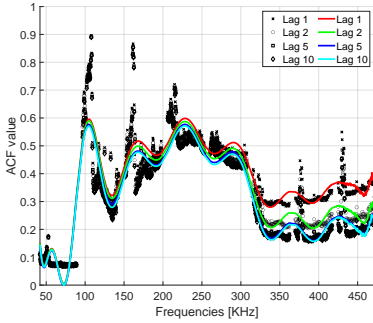


(b) Location 2

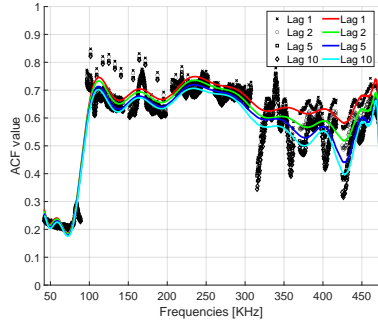


(c) Location 3

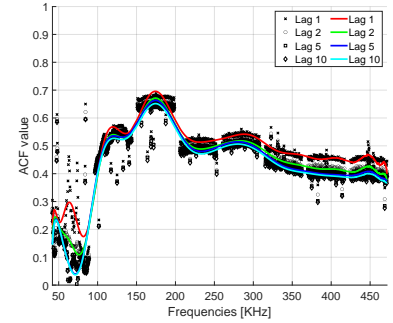
Fig. 7: Fraction of stationary chunks as a function of chunk length and the three considered locations.



(a) Location 1



(b) Location 2



(c) Location 3

Fig. 8: Autocorrelation (ACF) values at lags 1, 2, 5, and 10 as a function of the frequency for the three considered locations. We also consider the interpolations of the aforementioned values with the solid red, green, blue and cyan lines, respectively.

Moreover, we checked the independence of the noise samples by resorting to the Ljung-Box Q-test, being defined as:

- $H_0$ : samples are independently distributed,
- $H_1$ : samples are not independently distributed.

while the test statistic is defined according to Eq. 1.

$$Q(T, L, k) = T(T + 2) \sum_{k=1}^L \frac{\rho(k)^2}{T - k} \quad (1)$$

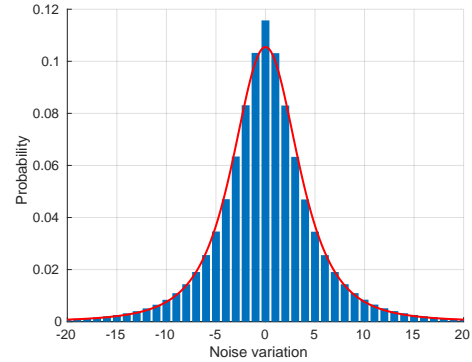
where  $T$  is the sample size,  $L$  is the number of autocorrelation lags, and finally,  $\rho(k)$  is the autocorrelation value at lag  $k$ . Under  $H_0$ , the statistic  $Q(T, L, k)$  asymptotically follows a  $\chi_L^2$  distribution with  $L$  degrees of freedom, and therefore the null hypothesis can be rejected if  $Q(T, L, k) > \chi_{1-\alpha, L}^2$ , i.e., the statistic is strictly greater than the  $1 - \alpha$  quantile of the  $\chi_L^2$  distribution, where  $\alpha$  the level of significance.

We evaluated  $Q(T, L, k) > \chi_{1-\alpha, L}^2$ , with  $L = 10$  s and  $\alpha = 0.05$ , and the test confirmed that the null hypothesis ( $H_0$ ) could be rejected for all the lags at all the frequencies. Therefore, we concluded that consecutive noise values (up to 10) were not independent while being correlated, as was also confirmed by the previous analysis in Fig. 8.

## VI. MODELING AND FORECASTING

We considered the sequence of noise samples  $n(t)$ , and we computed the difference between consecutive values, i.e.,

$d(t) = n(t) - n(t - 1)$ , with  $t > 1$ . The blue bars in Fig. 9 show the probability distribution function associated with the noise variation  $d(t)$  computed over consecutive noise samples considering all the frequencies and all the locations.

Fig. 9: Empirical distribution (blue bars) associated with the differentiate of two consecutive noise values  $d(t) = n(t) - n(t - 1)$ , and the  $t$  scale-distribution being the best-fit according to the maximum likelihood criteria.

We performed a best-fit (maximum-likelihood) over the empirical distribution by considering several well-known distributions. We found that the best-fit was represented by the

$t$  location-scale with a location parameter  $\mu = 1.8 \cdot 10^{-3}$ , scale parameter  $\sigma = 3.47$ , and shape parameter  $\nu = 2.87$ . The solid red line in Fig. 9 shows the  $t$  location-scale function with the aforementioned parameters.

Figure 9 proves that the vast majority of the noise samples kept the same value as the previous one (approximately 12% of the cases), while more than 30% of the samples is affected by minor variations, i.e.,  $\pm 1$ . These findings confirm the results obtained by the autocorrelation (recall Fig. 8), where we observed a significant correlation at lag 1 and 2.

Our measurements, and the related analysis, prove that noise samples can be considered a stationary process, highly correlated, and very “slow”, i.e., the noise process is characterized by a persistent mean value that is affected by small fluctuations, i.e., less than  $\pm 2dB\mu V$  in 50% of the cases.

**Steady-state analysis.** In the following, we consider the duration of steady-state (burst) periods in the sequences of the collected noise values. As for the previous analysis, for each location, we computed the derivative associated with all the noise samples (by considering the frequencies all together), and we investigated different levels of variations by considering the following cases:

- $\frac{d}{dt}n(t) = 0$ : Adjacent noise samples with the same value.
- $\frac{d}{dt}n(t) \leq 1$ : Adjacent noise samples with derivative values not exceeding 1.
- $\frac{d}{dt}n(t) \leq 2$ : Adjacent noise samples with derivative values not exceeding 2.
- $\frac{d}{dt}n(t) \leq 3$ : Adjacent noise samples with derivative values not exceeding 3.

The objective of this analysis was to investigate the frequencies of abrupt changes in the noise process, or to assess the length of (almost) steady periods in the sequence of the noise values. Figures 10 show the four aforementioned cases in the three locations. First, we observe that the three locations are characterized by similar trends, although there are peculiarities due to the different number of occurrences, which might have been due to either the location or the superposition of all the frequencies. Moreover, we observe a strong linear relation starting at a burst length equal to 2 s up to a burst length equal to 100 s. Given the log-log scale nature of the plot, we highlighted the geometric distribution nature of the process where bursts of length  $k$  were constituted by independent  $k$  events with derivative less or equal than  $D$ , with  $D$  being 0, 1, 2, and 3. We note that the independence is related to the values of the derivative and not (as previously discussed) to the absolute values of the noise process, which in turn are characterized by a strong correlation.

## VII. DISCUSSION

We considered several aspects associated with noise samples collected from the NB-PLC frequency spectrum. The overall number of collected samples sums to 1,826,665,200, with 690,019,200, 516,466,800, and 620,179,200, collected at locations 1, 2, and 3, respectively. We firstly verified that the sampling period was consistent during the long measurement period (approximately 10 days) by considering the probability mass function (and the related cumulative probability) associated with the derivative of the sampling period (recall Fig. 3).

We started our analysis by looking at the overall NB-PLC spectrum, i.e., eight channels constituted of 776 frequencies in the range between 41,992 Hz and 471,680 Hz (recall Fig. 4). The baseline statistics (minimum, maximum, quantiles 10, 50, and 90) highlight the patterns that are common to the three locations and some significant differences. Indeed, the average noise level is higher in channel 1 independently of the location, and after an abrupt attenuation between channel 1 and 2, the noise level decreases toward the higher frequencies. It is worth noting that this phenomenon affects all the aforementioned statistics independently of the location. Conversely, each location is affected by peculiar noise patterns such as spikes, or higher/lower noise values at specific frequency values.

We then moved to evaluating the stationarity of the noise process (Fig. 7). We searched the traces for chunks (of different sizes) having stationarity properties (testing negative to the unit root test). We verified that when the chunk length increased, the noise samples of the chunks tended to be less stationary. Channels behave in the same way independently of the the locations, apart from the anomaly of channel 1 in locations 2 and 3 (recall Fig. 7b and Fig. 7c). We noted that a chunk length of 30 samples (lasting 30 s) has a probability of greater than 90% of being stationary.

Moreover, we considered the ACF as a function of frequency and location. We evaluated the ACF at lags 1, 2, 5, and 10, and as for the previous analysis, we found common patterns at all the locations. While we observed that some channels could experience lower ACF values, i.e., channel 1, all the considered lags exhibit a high correlation at all the frequencies and independently of location.

Finally, we considered a model for the noise process (Fig. 9). We computed the derivative for all the noise samples and we searched for a best-fit according to several distributions: we evaluated the  $t$ -location scale as the distribution having the best fit to our data. We observed that approximately 50% of adjacent values exhibited a derivative value between -3 and 3, therefore, we analyzed further the distribution of consecutive samples, considering the samples that featured the same derivative values (Fig. 10). We showed that consecutive noise samples were not affected by large fluctuations; indeed, approximately 50% of our data  $n(t)$  was characterized by long bursts with  $\frac{d}{dt}n(t) \leq 3$ .

## VIII. CONCLUSION

We introduced a statistical description of the noise process in the NB-PLC frequency band. Our data collection involved more than 1.8 billion samples taken from three different locations over a time span of approximately 10 days. Our analysis focused on the noise time series from the NB-PLC bandwidth. First, we found a correlation (up to 30 s) at intra-frequency level. Moreover, we provided a thorough analysis involving stationarity, autocorrelation, and independence. Finally, we proved that the derivative of the noise process could be modeled according to a  $t$ -location scale distribution, while being characterized by sequence of values affected by small fluctuations, in the range of  $3dB\mu V$ .

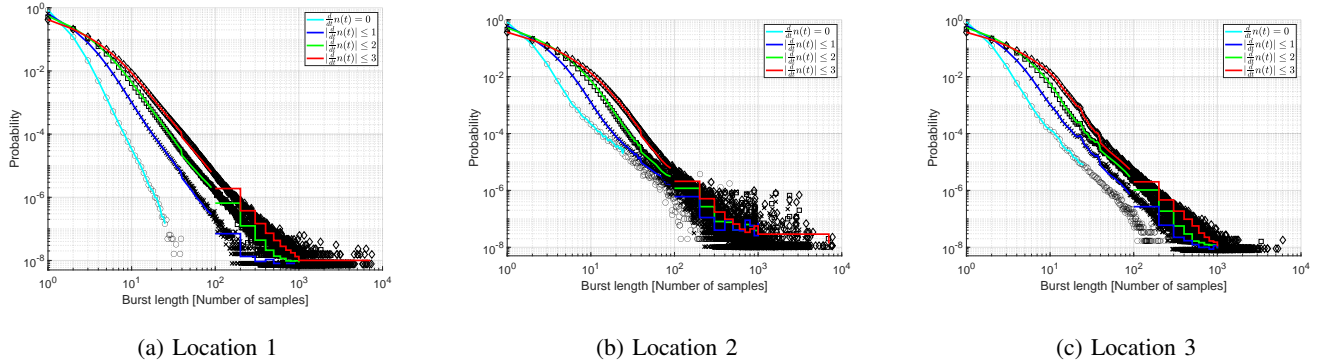


Fig. 10: Steady-state analysis of the noise process: we consider different derivative values  $D \in \{0, 1, 2, 3\}$  and count for how many subsequent noise samples (bursts) feature  $\frac{d}{dt}n(t) \leq D$ .

#### ACKNOWLEDGMENT

This publication was made possible by NPRP grant NPRP12S-0125-190013 from the Qatar National Research Fund (a member of Qatar Foundation). The findings achieved herein are solely the responsibility of the authors.

#### REFERENCES

- [1] C. Cano, A. Pittolo, D. Malone, L. Lampe, A. M. Tonello, and A. G. Dabak, "State of the art in power line communications: From the applications to the medium," *IEEE Journal on Selected Areas in Communications*, vol. 34, no. 7, pp. 1935–1952, July 2016.
- [2] S. Galli, A. Scaglione, and Z. Wang, "For the grid and through the grid: The role of power line communications in the smart grid," *Proceedings of the IEEE*, vol. 99, no. 6, pp. 998–1027, June 2011.
- [3] A. Sendin, I. Peña, and P. Angueira, "Strategies for power line communications smart metering network deployment," *Energies*, vol. 7, no. 4, pp. 2377–2420, 2014.
- [4] N. Andreadou, M. Guardiola, and G. Fulli, "Telecommunication technologies for smart grid projects with focus on smart metering applications," *Energies*, vol. 9, no. 5, p. 375, 2016.
- [5] M. R. Fliss, J. Hernandez Fernandez, A. Omri, and G. Oliveri, "NB-PLC successful transmission probability analysis," in *2019 2nd International Conference on Smart Grid and Renewable Energy (SGRE)*, 2019, pp. 1–6.
- [6] A. Omri, J. Hernandez Fernandez, A. Sanz, and M. R. Fliss, "PLC channel selection schemes for ofdm-based NB-PLC systems," in *2020 IEEE International Symposium on Power Line Communications and its Applications (ISPLC)*, 2020, pp. 1–6.
- [7] M. Zimmermann and K. Dostert, "An analysis of the broadband noise scenario in powerline networks," in *International Symposium on Power-line Communications and its Applications (ISPLC2000)*, 2000, pp. 5–7.
- [8] N. Andreadou and F.-N. Pavlidou, "Modeling the noise on the ofdm power-line communications system," *IEEE Transactions on Power Delivery*, vol. 25, no. 1, pp. 150–157, 2009.
- [9] G. Laguna-Sanchez and M. Lopez-Guerrero, "On the use of alpha-stable distributions in noise modeling for PLC," *IEEE Transactions on Power Delivery*, vol. 30, no. 4, pp. 1863–1870, 2015.
- [10] T. Rappaport, *Wireless Communications: Principles and Practice*, 2nd ed. USA: Prentice Hall PTR, 2001.
- [11] Cybersecurity Research and Innovation Laboratory, "NB-PLC noise measurement dataset from three different locations."
- [12] M. Katayama, T. Yamazato, and H. Okada, "A mathematical model of noise in narrowband power line communication systems," *IEEE Journal on Selected areas in Communications*, vol. 24, no. 7, pp. 1267–1276, 2006.
- [13] L. Di Bert, P. Caldera, D. Schwingshackl, and A. M. Tonello, "On noise modeling for power line communications," in *2011 IEEE International Symposium on Power Line Communications and Its Applications*. IEEE, 2011, pp. 283–288.
- [14] T. Shongwey, A. H. Vinck, and H. C. Ferreira, "On impulse noise and its models," in *18th IEEE International Symposium on Power Line Communications and Its Applications*. IEEE, 2014, pp. 12–17.
- [15] M. Nassar, A. Dabak, I. H. Kim, T. Pande, and B. L. Evans, "Cyclostationary noise modeling in narrowband powerline communication for smart grid applications," in *2012 IEEE International Conference on Acoustics, Speech and Signal Processing (ICASSP)*. IEEE, 2012, pp. 3089–3092.
- [16] M. Elgenedy, M. Sayed, A. El Shafie, I. H. Kim, and N. Al-Dhahir, "Cyclostationary noise modeling based on frequency-shift filtering in NB-PLC," in *2016 IEEE Global Communications Conference (GLOBECOM)*. IEEE, 2016, pp. 1–6.
- [17] M. Nassar, K. Gulati, Y. Mortazavi, and B. L. Evans, "Statistical modeling of asynchronous impulsive noise in powerline communication networks," in *2011 IEEE Global Telecommunications Conference-GLOBECOM 2011*. IEEE, 2011, pp. 1–6.
- [18] H. Gassara, F. Rouissi, and A. Ghazel, "A novel stochastic model for the impulsive noise in the narrowband indoor PLC environment," in *2015 IEEE International Instrumentation and Measurement Technology Conference (I2MTC) Proceedings*. IEEE, 2015, pp. 62–67.
- [19] G. Laguna-Sanchez and M. Lopez-Guerrero, "An experimental study of the effect of human activity on the alpha-stable characteristics of the power-line noise," in *18th IEEE International Symposium on Power Line Communications and Its Applications*. IEEE, 2014, pp. 6–11.
- [20] D. Umehara, H. Yamaguchi, and Y. Morihiro, "Turbo decoding in impulsive noise environment," in *IEEE Global Telecommunications Conference, 2004. GLOBECOM'04.*, vol. 1. IEEE, 2004, pp. 194–198.
- [21] H. Meng, Y. L. Guan, and S. Chen, "Modeling and analysis of noise effects on broadband power-line communications," *IEEE Transactions on Power Delivery*, vol. 20, no. 2, pp. 630–637, 2005.
- [22] M. H. Chan and R. W. Donaldson, "Amplitude, width, and interarrival distributions for noise impulses on intrabuilding power line communication networks," *IEEE Transactions on Electromagnetic Compatibility*, vol. 31, no. 3, pp. 320–323, 1989.
- [23] J. A. Cortés, A. Sanz, P. Estopinán, and J. I. García, "On the suitability of the middleton class a noise model for narrowband plc," in *2016 International Symposium on Power Line Communications and its Applications (ISPLC)*. IEEE, 2016, pp. 58–63.
- [24] P. A. TWG, "Specification for Powerline Intelligent Metering Evolution," *R1.4*, October 2014.
- [25] M. T. Inc., *PL360-EK Host Controller*, 2019.
- [26] —, *PL360-EK User Guide*, 2018.
- [27] D. Kwiatkowski, P. C. Phillips, and P. Schmidt, "Testing the Null Hypothesis of Stationarity Against the Alternative of a Unit Root: How Sure Are We That Economic Time Series Have a Unit Root?" Cowles Foundation for Research in Economics, Yale University, Cowles Foundation Discussion Papers 979, May 1991.